

Adaptive host-guest chiral recognition in a nanoarchitectonics with biomimetic MOF mimicking DNA

Xiaohui Niu, ^{*[a]} Rui Zhao, ^[a] Yongqi Liu, ^[a] Mei Yuan, ^[a] Hongfang Zhao, ^[a] Hongxia Li, ^[a] Xing
Yang, ^[b] Hui Xu, ^[a] Kunjie Wang^{*[a]}

* Corresponding Author: wangkj80@163.com (Wang.K.J.); 18893700891@163.com (Niu.X.H.)

^a College of Petrochemical Technology, Lanzhou University of Technology, 730050, Lanzhou, PR
China.

^b School of Materials Science and Engineering, Lanzhou Jiaotong University, 730070, Lanzhou, PR
China.

Table of Contents

1. Results and discussion.....	S1-S23
2. References.....	S24

1. Results and discussion:

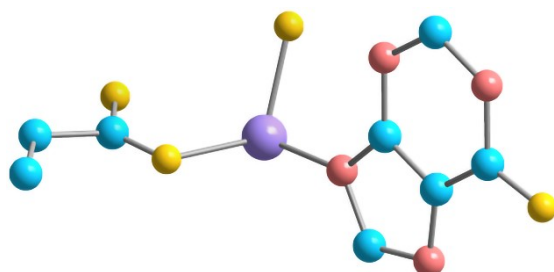


Figure S1. The asymmetric unit.

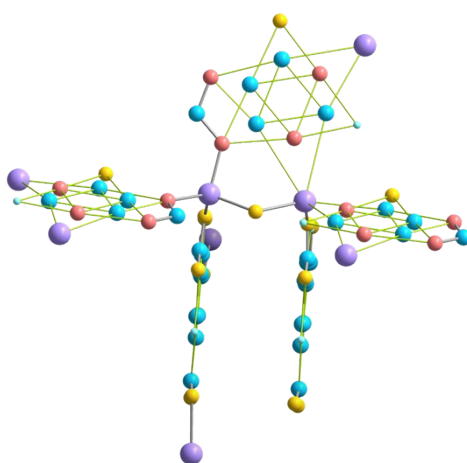


Figure S2. The coordination environment of the ZnBTCHx.

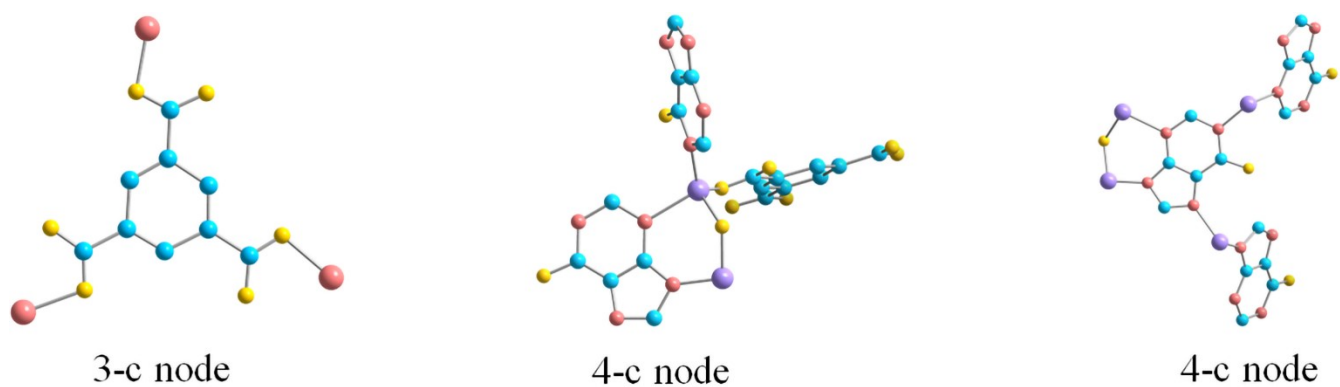


Figure S3. Zn_2O -cluster as a four-coordinated (4-c) node, hypoxanthine as a 4-c node, and BTC as a 3-c node, respectively.

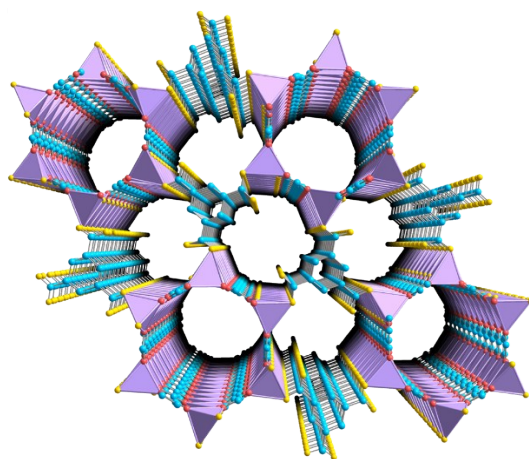


Figure S4. 3D framework of $ZnBTCHx$ with two types of 1-D channels.

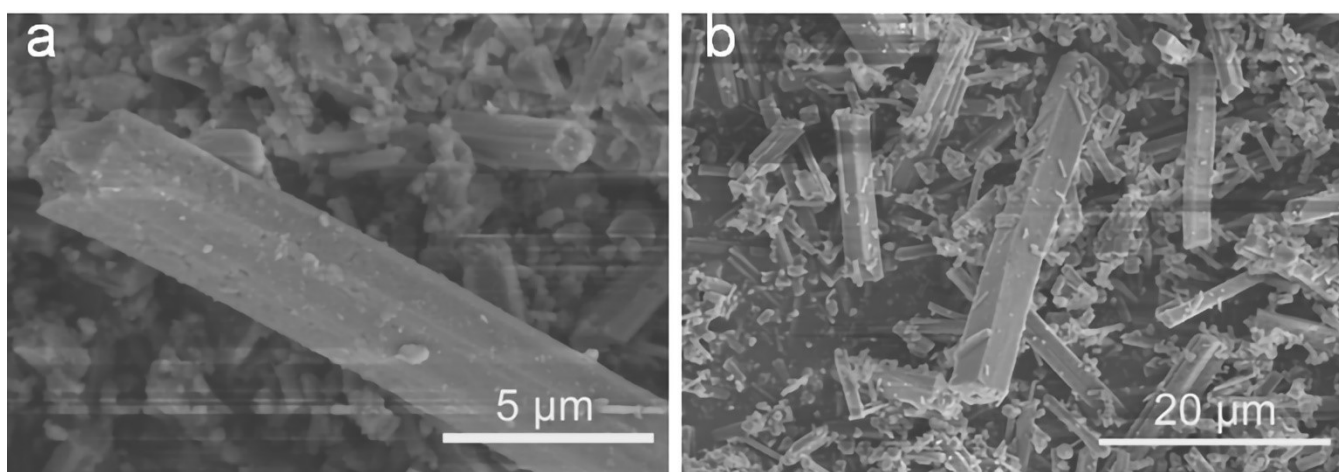


Figure S5. SEM of ZnBTCH_x.

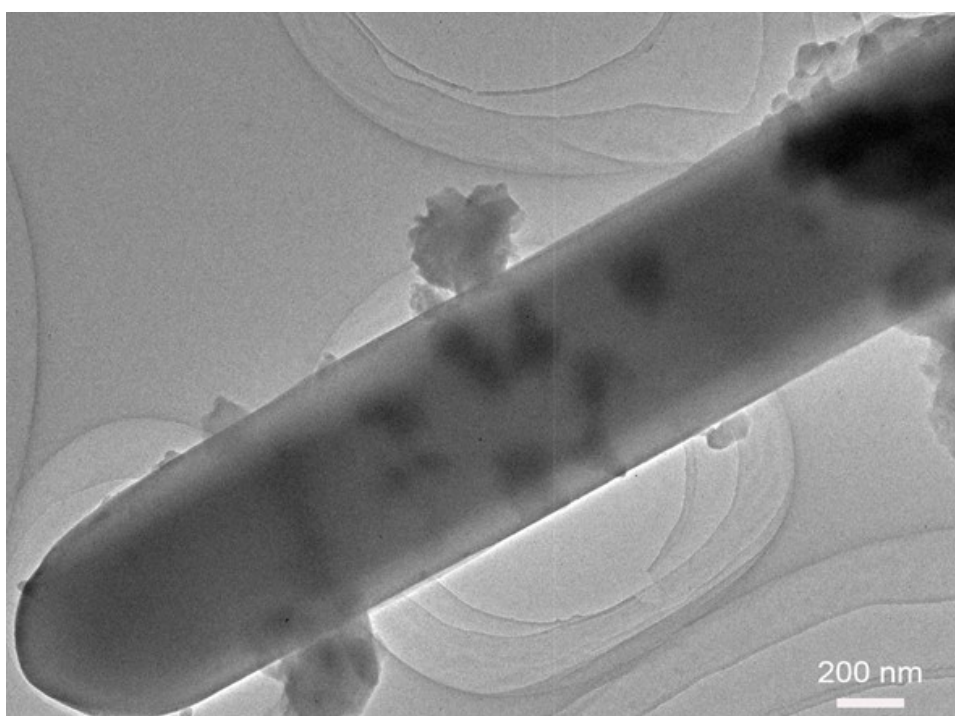


Figure S6. TEM of ZnBTCHx.

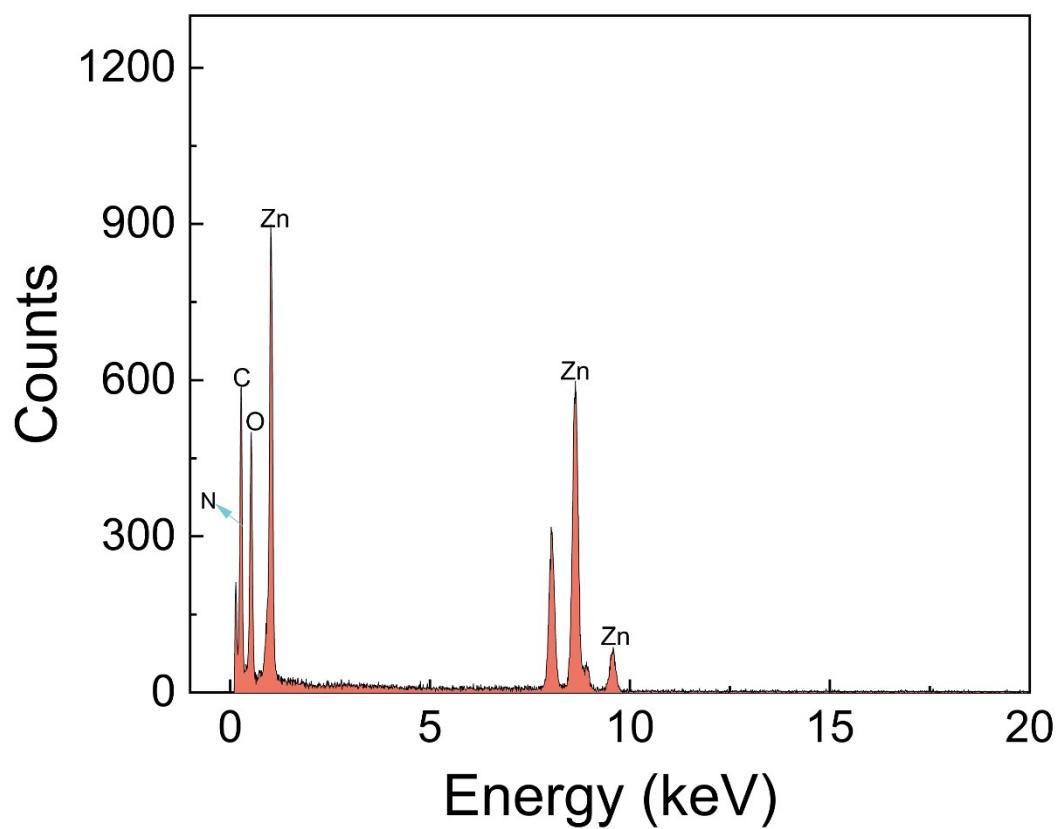


Figure S7. EDX survey spectra of ZnBTCHx.

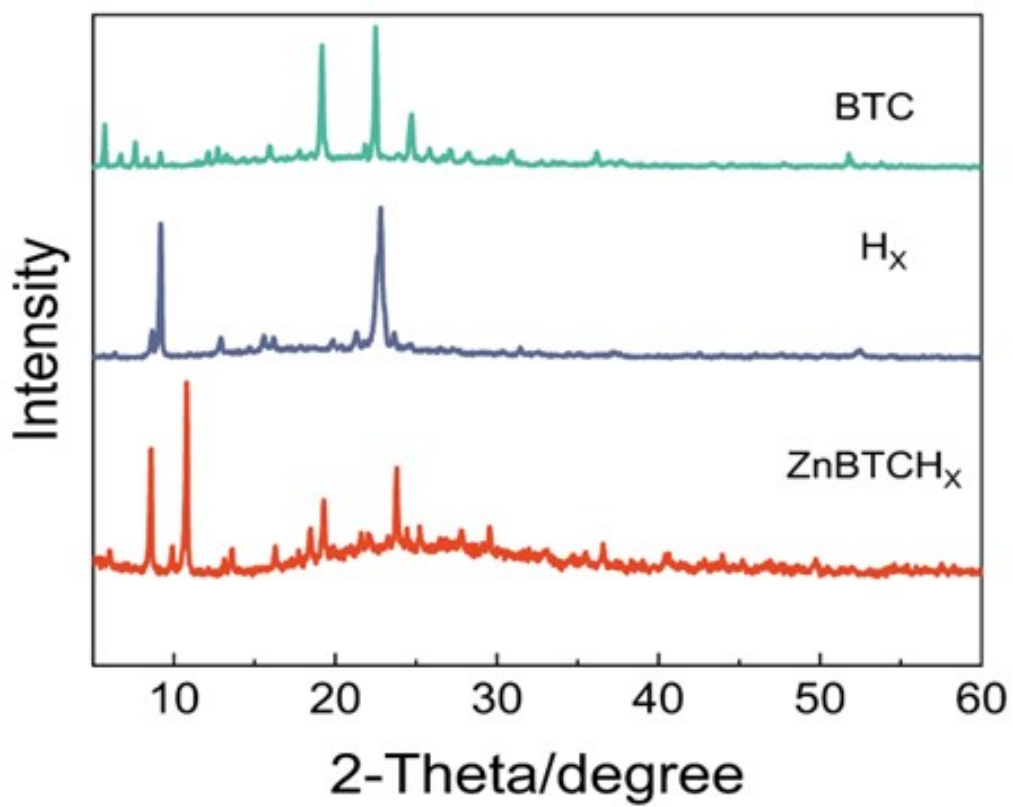


Figure S8. XRD profiles of BTC, H_x and ZnBTCH_x.

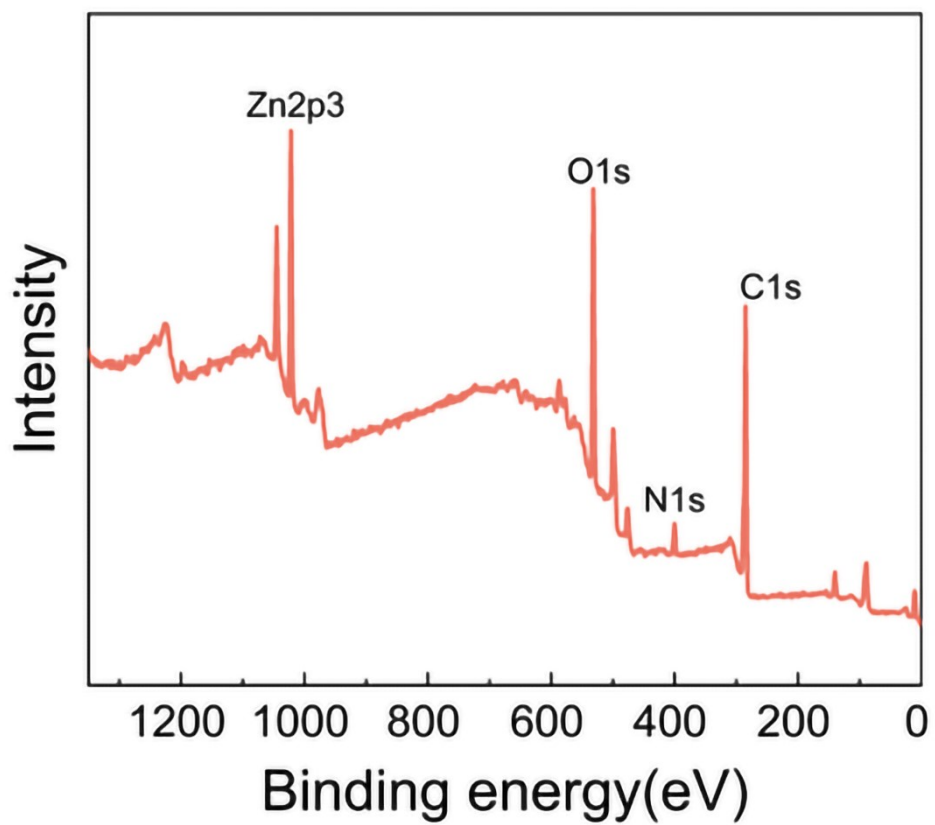


Figure S9. XPS survey spectra of ZnBTCH_x.

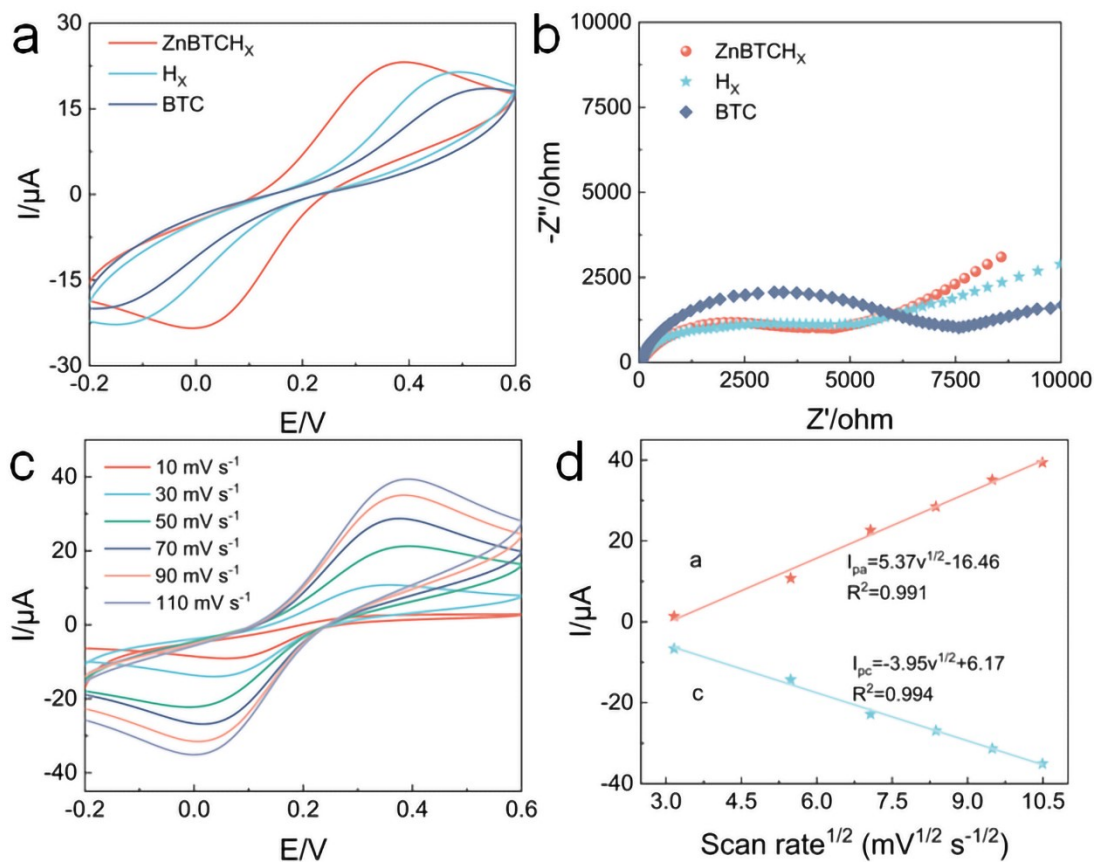


Figure S10. (a) CVs of BTC/GCE, H_x/GCE and ZnBTCH_x/GCE. (b) EIS of the BTC/GCE, H_x/GCE and ZnBTCH_x/GCE. (c) CVs of ZnBTCH_x/GCE at different scan rates (10 mVs^{-1} , 30 mVs^{-1} , 50 mVs^{-1} , 70 mVs^{-1} , and 90 mVs^{-1}). (d) Linear regression between scan rate and current value.

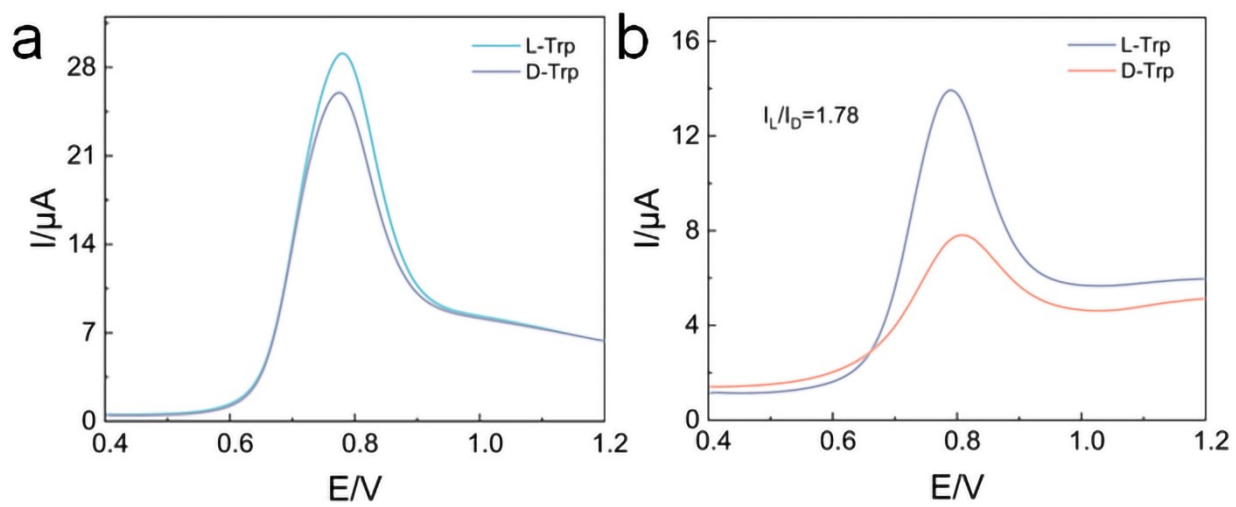


Figure S11. DPV curves recorded for detecting Trp enantiomers using BTC(a), Hx(b) electrodes.

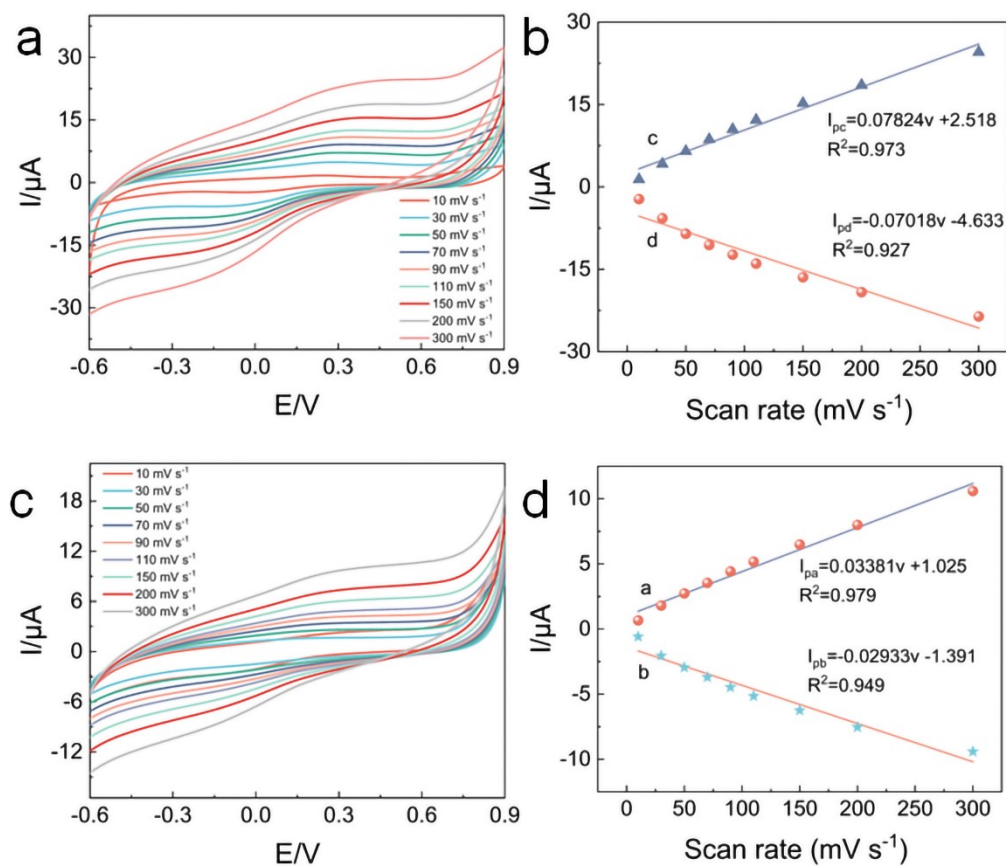


Figure S12. (a) CVs of ZnBTCHX/GCE in L-Trp solution at different scan rates. (b) Linear regression between scan rate and current value. (c) CVs of ZnBTCHX/GCE in D-Trp solution at different scan rates. (d) Linear regression between scan rate and current value.

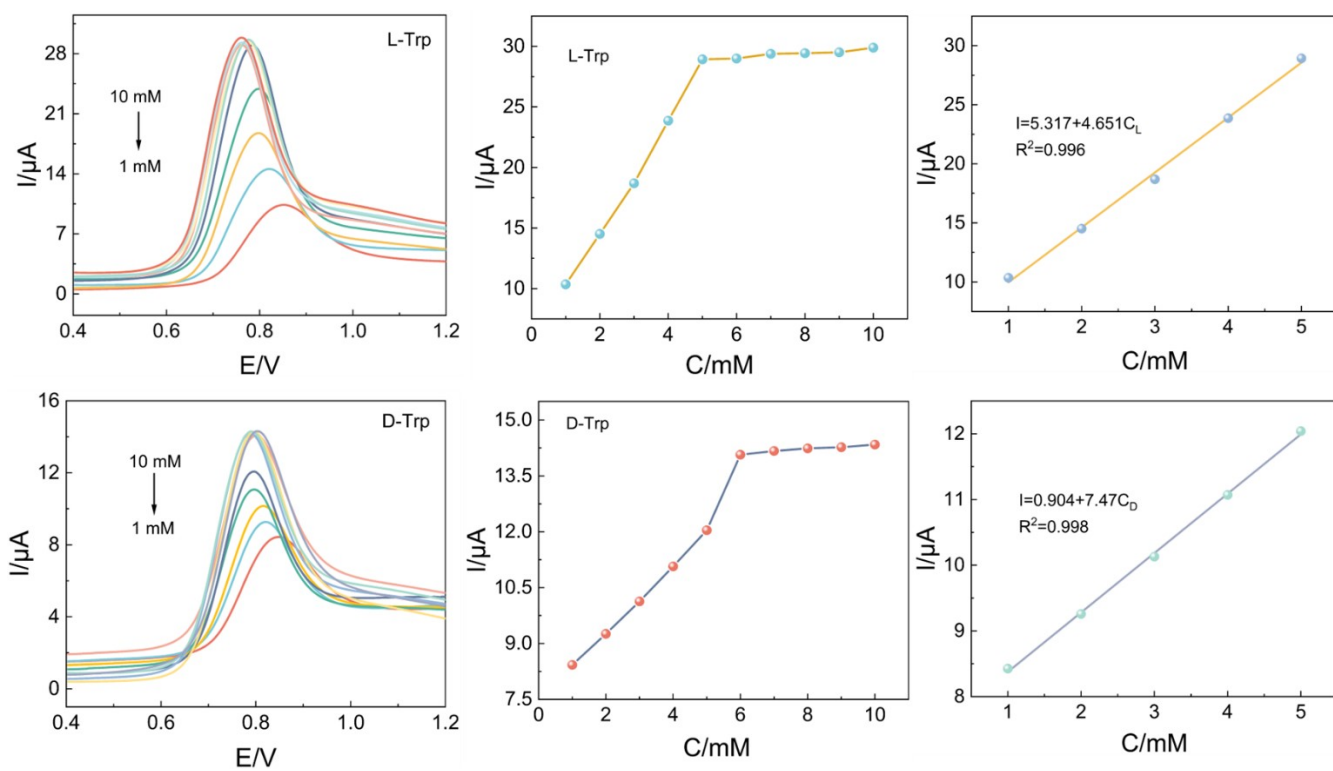


Figure S13. DPVs of L-Trp and D-Trp with different concentrations from 1-10 mM and Linear range.

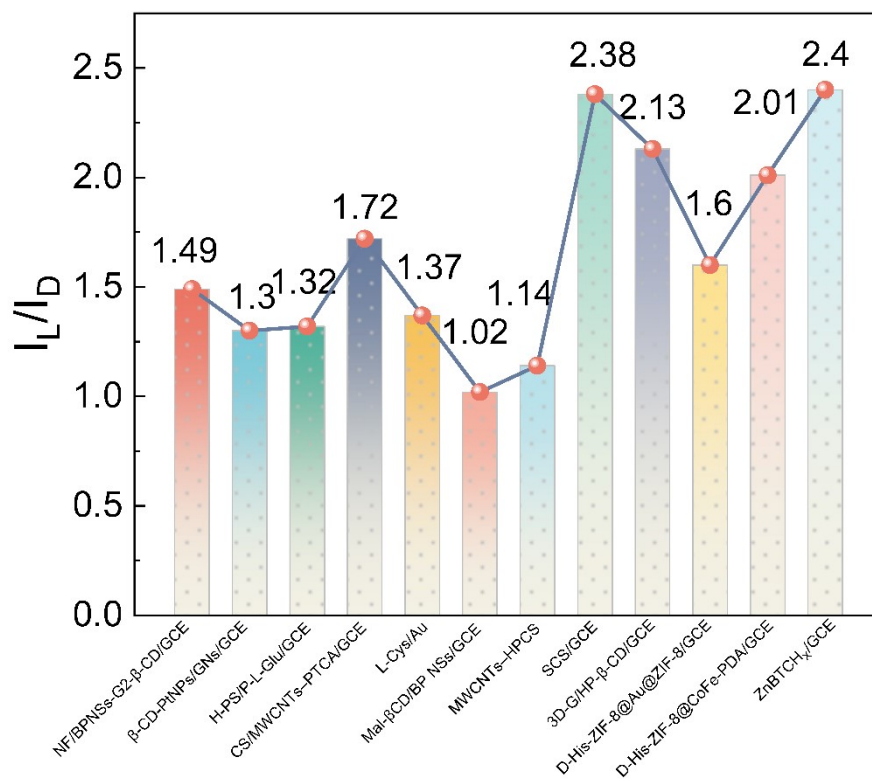


Figure S14. Comparison of different modified electrodes in the recognition efficiency of Trp enantiomers.

Electrochemical sensors	pH	Recognition efficiency	LOD	Ref
NF/BPNSs-G2-β-CD/GCE	7	1.49	L-Trp (1.07 μM)	1
β-CD-PtNPs/GNs/GCE	7	1.30	L-Trp (1.7× 10 ⁻⁵ M)	2
H-PS/P-L-Glu/GCE	7	1.32	-	3
CS/MWCNTs-PTCA/GCE	-	1.72	-	4
L-Cys/Au	5.4	1.37	-	5
Mal-βCD/BP NSs/GCE	7	1.02	-	6
MWCNTs-HPCS	7	1.14	-	7
SCS/GCE	7	2.38	-	8
3D-G/HP-β-CD/GCE	7	2.13	-	9
D-His-ZIF-8@Au@ZIF-8/GCE	5.5	1.6	-	10
D-His-ZIF-8@CoFe-PDA/GCE	6	2.01	L-Trp (0.066 mM)	11
ZnBTCH _x /GCE	6	2.40	L-Trp (0.031 mM)	This work

Table S1 Comparison of different modified electrodes in the recognition efficiency of Trp enantiomers.

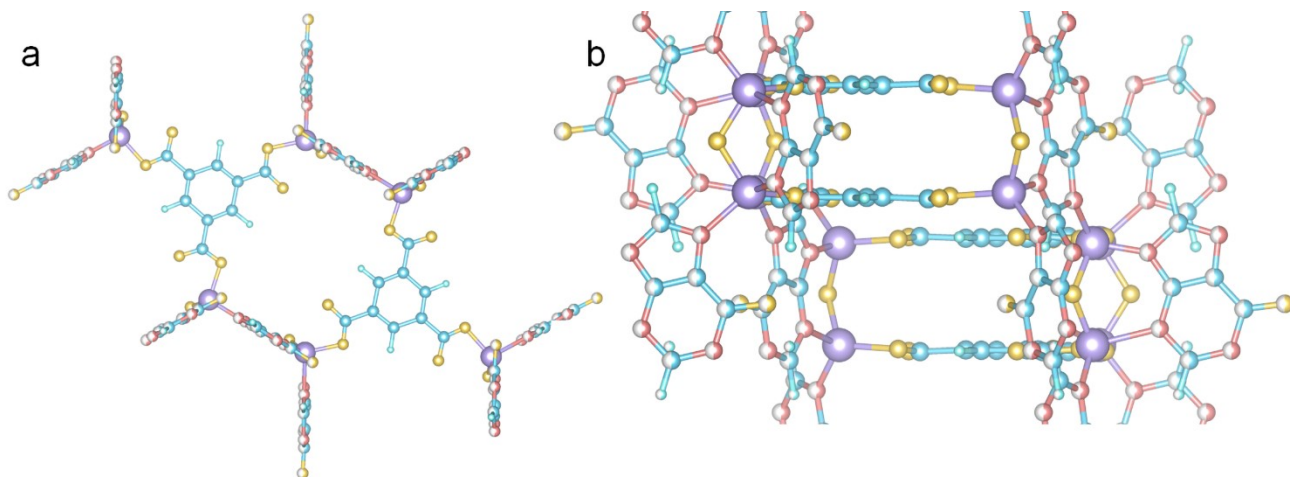


Figure S15. (a) Top view and (b) side view of ZnBTCHx.

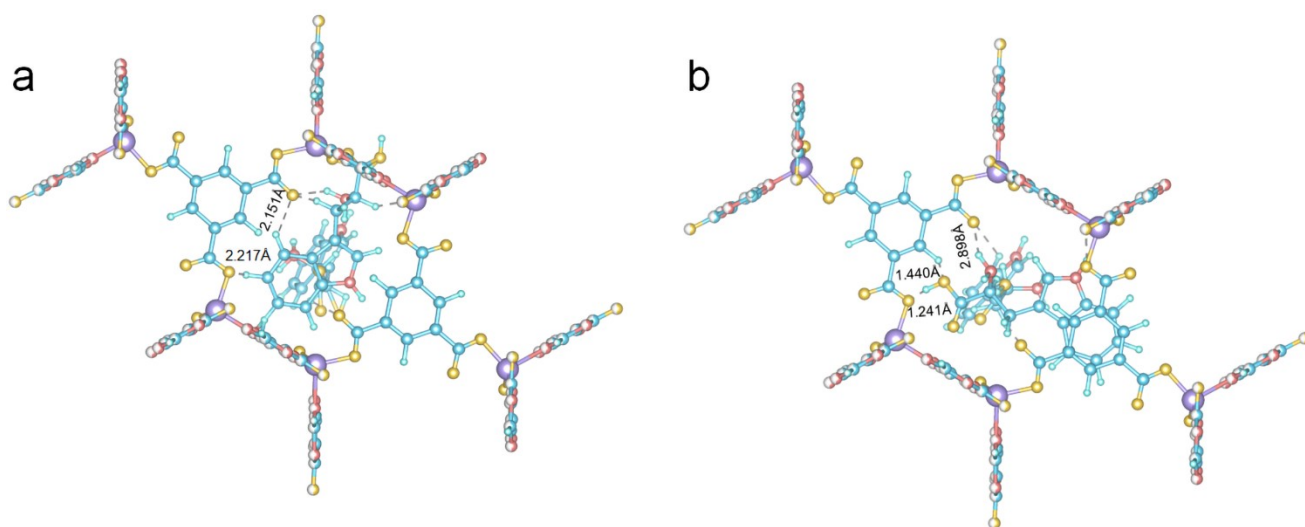


Figure S16. The bond length of (a) D-Trp@ZnBTCHx and (b) L-Trp@ZnBTCHx.

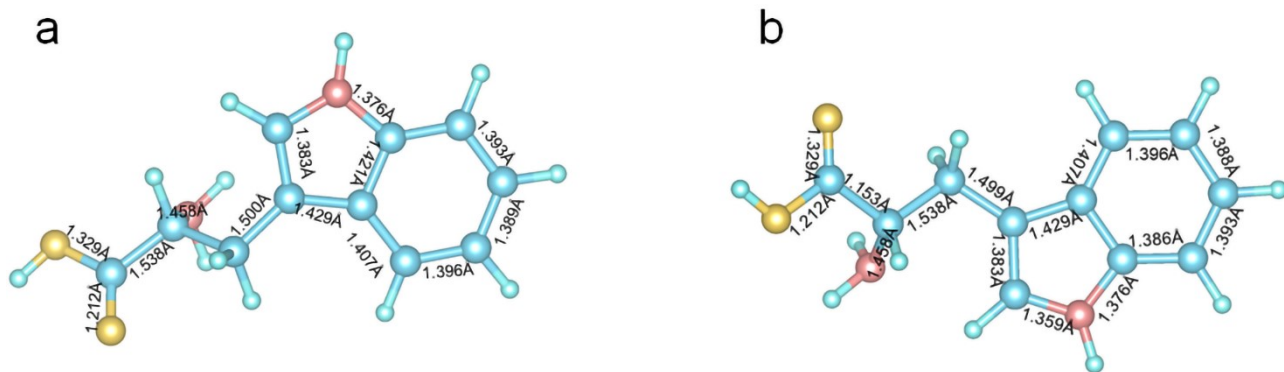


Figure S17. The bond length of (a) D-Trp and (b) L-Trp.

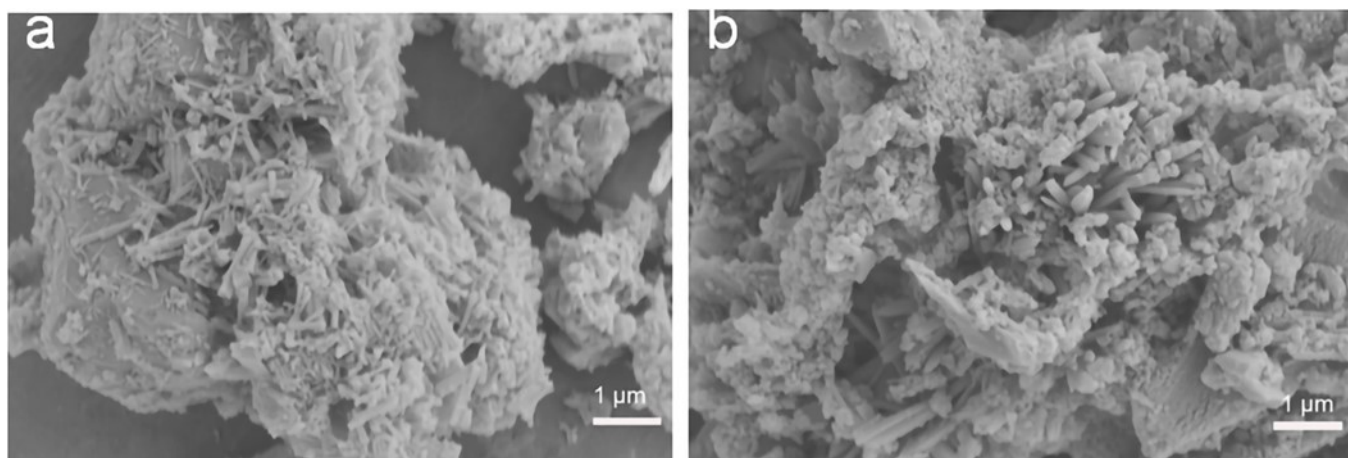


Figure S18. (a, b) SEM of L-Trp@ZnBTCHx and D-Trp@ZnBTCHx.

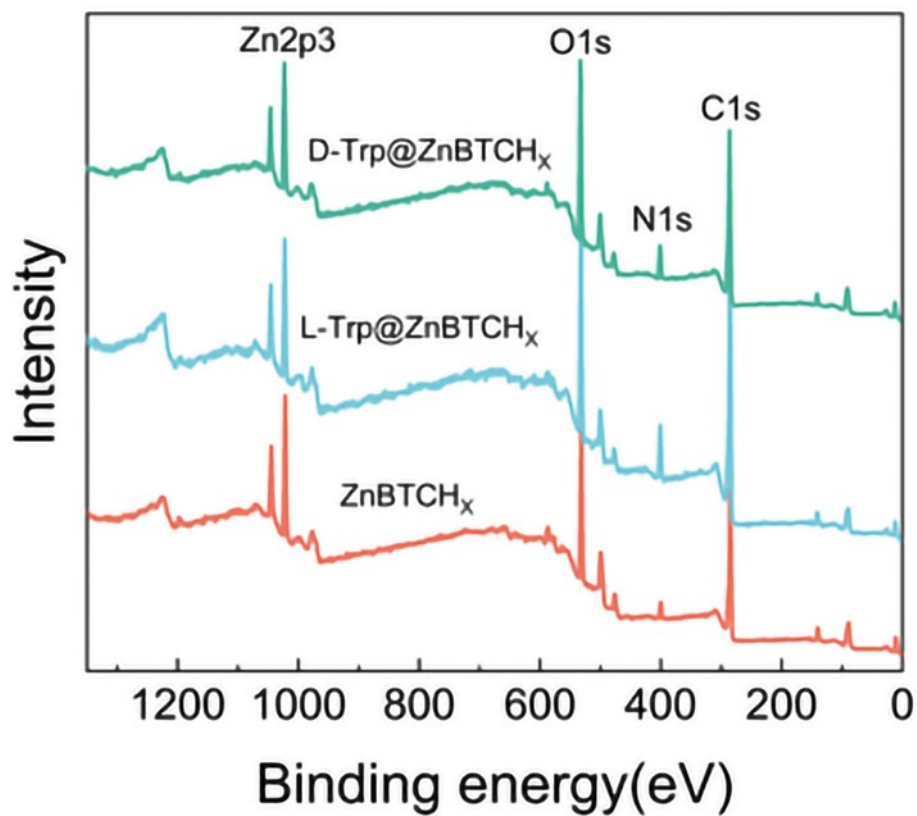


Figure S19. XPS of L-Trp@ZnBTCH_x and D-Trp@ZnBTCH_x.

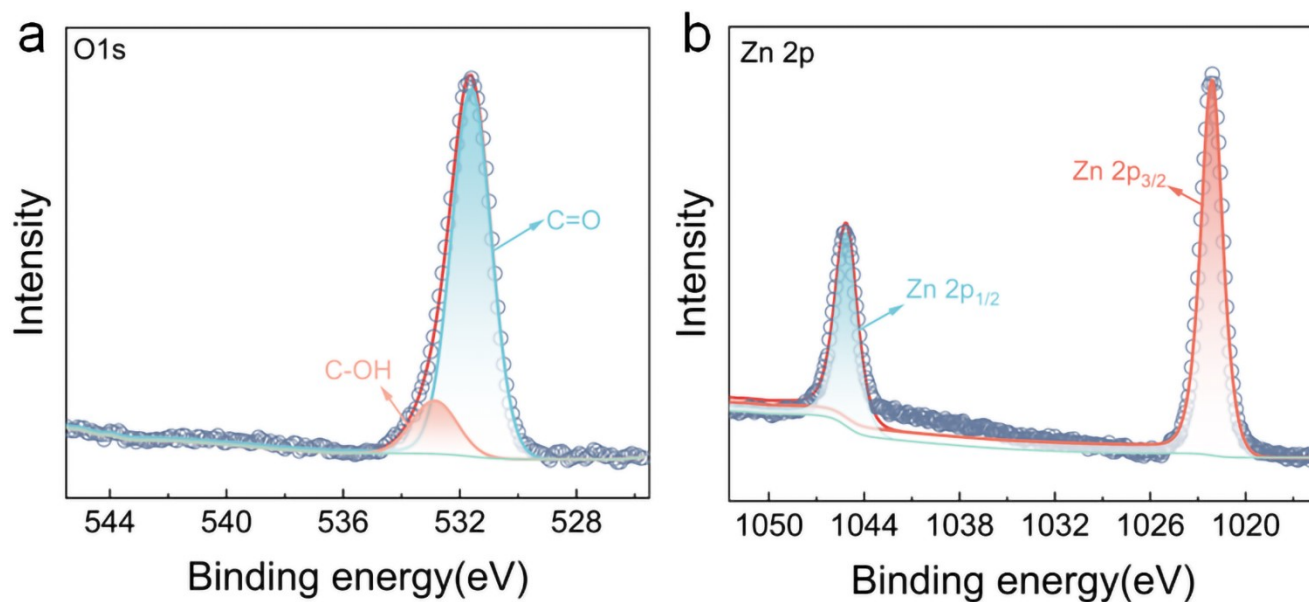


Figure S20. (a, b) O1s XPS spectrum (a) and Zn 2p XPS spectrum (b) recorded for L-Trp@ZnBTCHx.

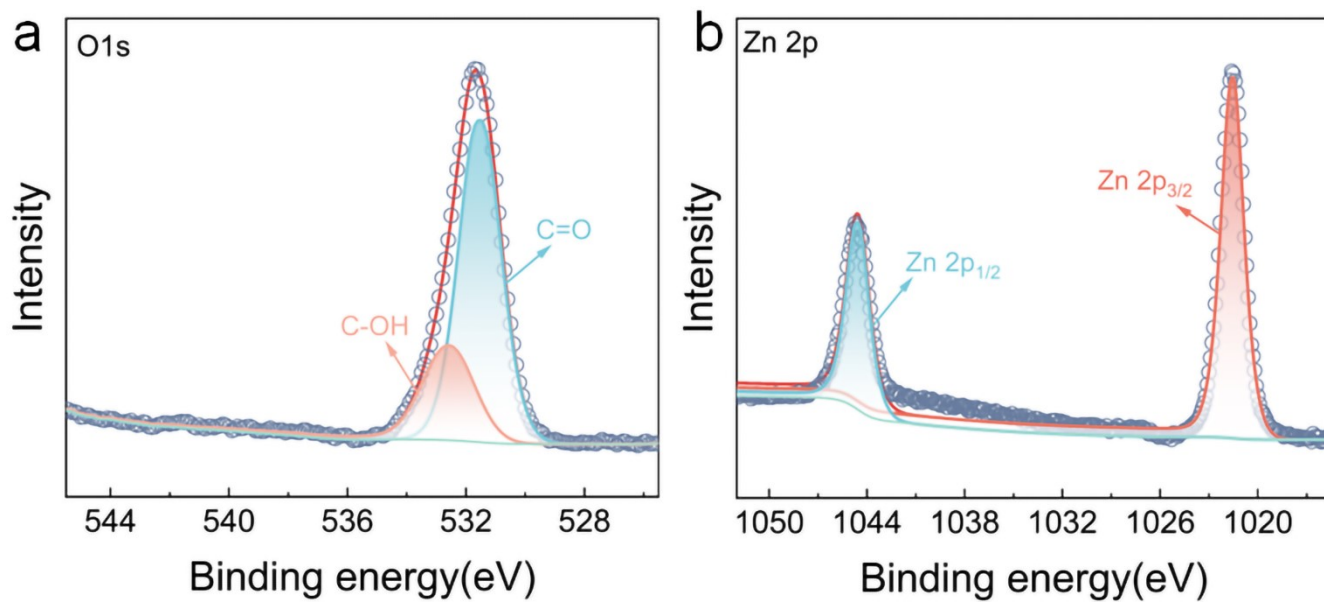


Figure S21. (a, b) O1s XPS spectrum (a) and Zn 2p XPS spectrum (b) recorded for D-Trp@ZnBTCHx.

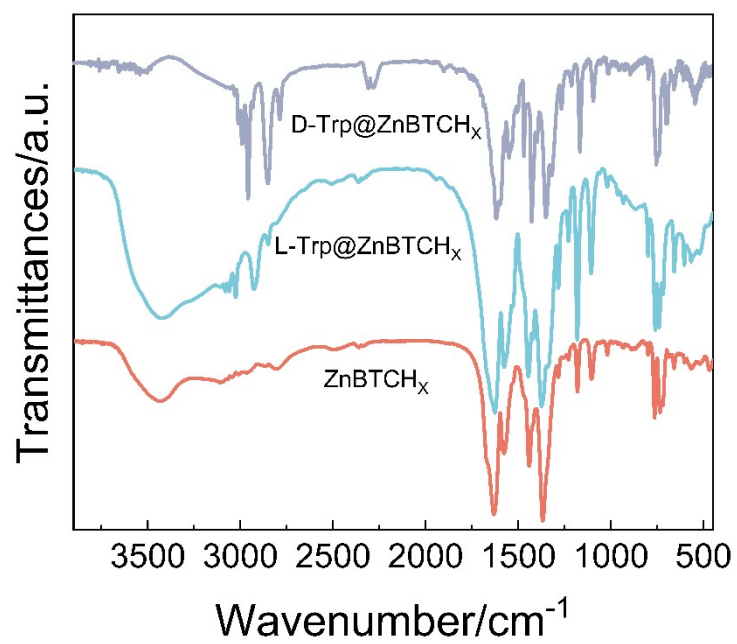


Figure S22. FT-IR spectra of L-Trp@ZnBTCH_x and D-Trp@ZnBTCH_x.

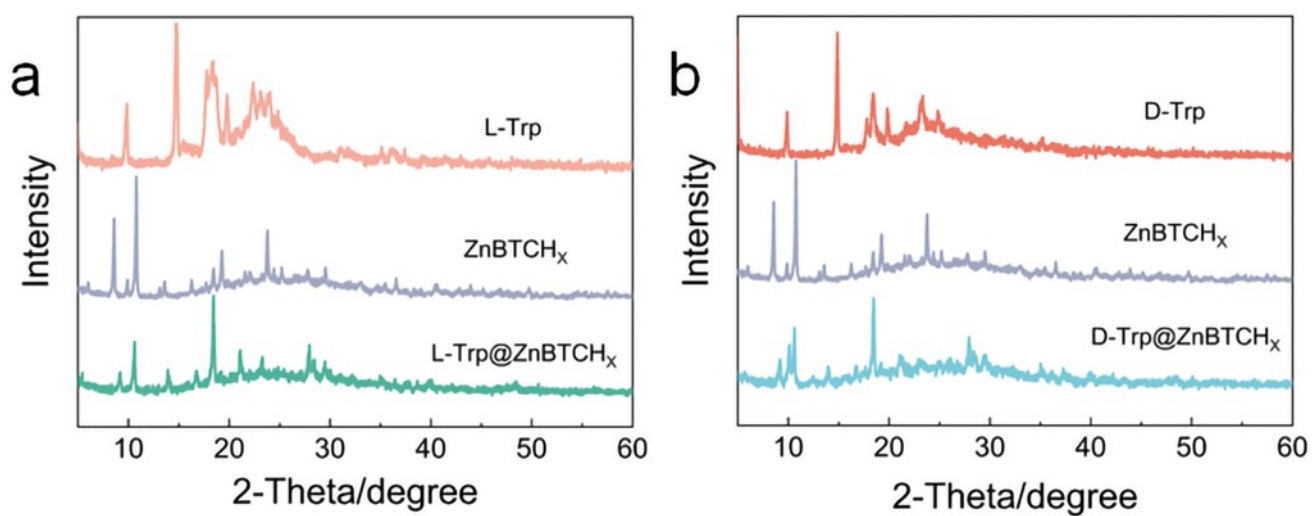


Figure S23. XRD profiles of L-Trp@ZnBTCH_x and D-Trp@ZnBTCH_x.

2. References

1. J. Zou and J. G. Yu, *Mater Sci Eng C Mater Biol Appl*, 2020, **112**, 110910.
2. J. Xu, Q. Wang, C. Xuan, Q. Xia, X. Lin and Y. Fu, *Electroanalysis*, 2016, **28**, 868-873.
3. L. Bao, Y. Tao, X. Gu, B. Yang, L. Deng and Y. Kong, *Electrochemistry Communications*, 2016, **64**, 21-25.
4. P. Jing, Z. Z. Yin, W. Cai, J. Li, D. Wu and Y. Kong, *Bioelectrochemistry*, 2022, **146**, 108110.
5. Q. Chen, J. Zhou, Q. Han, Y. Wang and Y. Fu, *Colloids Surf B Biointerfaces*, 2012, **92**, 130-135.
6. J. Zou, X. W. Lan, G. Q. Zhao, Z. N. Huang, Y. P. Liu and J. G. Yu, *Mikrochim Acta*, 2020, **187**, 636.
7. Z. Li, Z. Mo, S. Meng, H. Gao, X. Niu, R. Guo and T. Wei, *RSC Advances*, 2017, **7**, 8542-8549.
8. X. Gu, Y. Tao, Y. Pan, L. Deng, L. Bao and Y. Kong, *Anal Chem*, 2015, **87**, 9481-9486.
9. W. Liang, Y. Rong, L. Fan, W. Dong, Q. Dong, C. Yang, Z. Zhong, C. Dong, S. Shuang and W.-Y. Wong, *Journal of Materials Chemistry C*, 2018, **6**, 12822-12829.
10. X. Niu, S. Yan, R. Zhao, H. Li, X. Liu and K. Wang, *ACS Applied Materials & Interfaces*, 2023, **15**, 22435-22444.
11. X. Niu, R. Zhao, S. Yan, H. Li, J. Yang, K. Cao, X. Liu and K. Wang, *Microchimica Acta*, 2023, **190**.